Daple deficiency causes hearing loss in adult mice by inducing defects in cochlear stereocilia and apical microtubules

Yoshiyuki Ozono
Osaka University
Atsushi Tamura (atamura@biosci.med.osaka-u.ac.jp)
Osaka University
Shogo Nakayama
Osaka University
Elisa Herawati
Sebelas Maret University
Yukiko Hanada
Osaka University
Kazuya Ohata
Osaka University
Maki Takagishi
Nagoya University
Masahide Takahashi
Nagoya University
Takao Imai
Osaka University
Yumi Ohta
Osaka University
Kazuo Oshima
Osaka University
Takashi Sato
Osaka University
Hidenori Inohara
Osaka University
Sachiko Tsukita
Osaka University

Research Article

Keywords: Daple deficiency, hearing loss, cochlear stereocilia, apical microtubules

Posted Date: March 3rd, 2021

DOI: https://doi.org/10.21203/rs.3.rs-263011/v1

Daple deficiency causes hearing loss in adult mice by inducing defects in cochlear stereocilia and apical microtubules

Yoshiyuki Ozono[1,2], Atsushi Tamura[1,3,4,*], Shogo Nakayama[1], Elisa Herawati[1,5], Yukiko Hanada[2,6], Kazuya Ohata[2,6], Maki Takagishi[7,+], Masahide Takahashi[7,8,+], Takao Imai[2,+], Yumi Ohta[2,+], Kazuo Oshima[2,+], Takashi Sato[2,+], Hidenori Inohara[2,+], and Sachiko Tsukita[1,3,4]

1. Laboratory of Biological Science, Graduate School of Frontier Biosciences and Graduate School of Medicine, Osaka University, 2-2 Yamadaoka, Suita, Osaka 565-0871, Japan.

2. Department of Otorhinolaryngology-Head and Neck Surgery, Graduate School of Medicine, Osaka University, 2-2 Yamadaoka, Suita, Osaka 565-0871, Japan.

3. Department of Pharmacology, Teikyo University, 2-11-1 Kaga Itabashi 173-8605, Tokyo, Japan.

4. Strategic Innovation and Research Center, Teikyo University, 2-11-1 Kaga Itabashi 173-8605, Tokyo, Japan.

5. Department of Biology, Faculty of Mathematics and Natural Science, Universitas Sebelas Maret Jalan Ir. Sutami 36 A, Surakarta, 57126, Indonesia.

6. Department of Neuroscience and Cell Biology, Graduate School of Medicine, Osaka University, 2-2 Yamadaoka, Suita, Osaka 565-0871, Japan.

7. Department of Pathology, Graduate School of Medicine, Nagoya University, 65 Tsurumai, Showa, Nagoya, Aichi 466-8550, Japan.

8. International Center for Cell and Gene Therapy, Fujita Health University, 1-98 Dengakugakubo, Kutsukake, Toyoake, Aichi, 470-1192, Japan

**corresponding.author* atamura@biosci.med.osaka-u.ac.jp

[+]these authors contributed equally to this work

ABSTRACT

The V-shaped arrangement of hair bundles on cochlear hair cells is critical for the auditory sensing. However, regulation of hair bundle arrangements is not fully understood. Recently, defects in hair bundle arrangement were reported in postnatal Dishevelled-associating protein (Daple)-deficient mice. Here, we found that adult *Daple*$^{-/-}$ mice exhibited hearing disturbances over a broad frequency range through auditory brainstem response testing. Consistently, distorted patterns of hair bundles were detected in almost all regions, more typically in the basal region of the cochlear duct. In adult *Daple*$^{-/-}$ mice, apical microtubules were irregularly aggregated, and the number of microtubules attached to plasma membranes was decreased. Similar phenotypes were manifested upon nocodazole treatment in a wild type cochlea culture without affecting the microtubule structure of the kinocilium. These results indicate critical roles of Daple in hair bundle arrangement, through the orchestration of apical microtubule distribution, and thereby in hearing, especially at high frequencies.

INTRODUCTION

The apical differentiation of epithelial cell sheets is critical for the functioning of organs. In the inner ear, the differentiation of stereociliary hair bundles in cochlear hair cells (HCs) is essential for hearing. All hair bundles in the cochlea form V-shaped vertices oriented in the same abneural (lateral) direction. Planar cell polarity (PCP) coordinates the alignment of cell polarities across a tissue plane at a cell-to-tissue level[1] [2]. However, our knowledge regarding the mechanisms underlying this coordination remains fragmentary. Dishevelled (Dvl)-associated protein (Daple, alternatively called ccdc88c), with a high leucine content, was first identified as a scaffold protein that interacts with Dvl, a core PCP protein[3] . Daple has been reported to regulate several biological activities, such as cell differentiation and proliferation, cell morphology, and cancer cell dynamics, at least partially through Frizzled-Gαi-related Wnt signals[4] [5] [6] [7]. Recently, deletion of *Daple* was shown to cause defects in the arrangement of hair bundles in the HCs of the organ of Corti (OC) in mice[8]. In *Daple*$^{-/-}$ mice, the dissociated localization of Gαi proteins and the primary cilium of HCs, kinocilium, has been reported to occur during the neonatal period and causes defects in the arrangement of hair bundles[8]. However, the hearing potential of mature cochlea was not analyzed in these mice. Furthermore, the multifaceted molecular mechanisms that connect deletion of *Daple* and defects in the arrangement of stereocilia remain at least partly elusive. Mice deficient in Lis-1, a dynein regulatory protein, also exhibit apical morphological deformities in HCs in the OC, similar to *Daple*$^{-/-}$ mice[9], suggesting the involvement of microtubules in the formation of apical structures in the HCs of the OC in the context of PCP. However, the role of apical microtubules in apical morphogenesis in HCs of the OC remains to be elucidated.

In this study, we analyzed, for the first time, Daple-deficient mice, from the neonate stage to the adult stage, to determine the role of Daple in HC apical morphogenesis, especially via microtubules. We show the presence of hearing disturbances at all frequencies examined using the auditory brainstem response (ABR) test, especially at high frequencies. Reflecting the ABR results, malformation of hair bundles was found to be more severe in the basal area, indicating that the PCP-related protein, Daple, plays a consistent role in the cochleae for hearing. Our findings also unravel the role of apical microtubules in HC apical differentiation, which is consistent with the results obtained upon nocodazole administration. Finally, Daple seems to be essential, especially during the morphogenesis of hair bundles, because malformation of hair bundles was consistent from birth to adulthood in Daple-deficient mice.

Results

Auditory brainstem response (ABR) testing revealed hearing defects in *Daple*$^{-/-}$ adult mice, especially at higher frequencies

Although *Daple*$^{-/-}$ mice, in the embryonic and neonatal stages, have previously been reported to have defects in the arrangement of hair bundles in cochlear HCs [8], hearing-potential and morphological changes with age have not been analyzed. Here, we performed ABR tests on 8–12-week-old mice and found lower sensitivity to sounds in *Daple*$^{-/-}$ mice than in *Daple*$^{+/+}$ mice at all frequencies, ranging from 4 to 32 kHz. A highly significant hearing disturbance was detected around 24 kHz (42.1 ± 9.1 in $^{+/+}$ vs. 74.3 ± 8.4 dB in $^{-/-}$, $p < 0.0001$, Fig. 1A). The gross shape and size of the cochleae in *Daple*$^{-/-}$ mice were comparable to those of the cochleae in *Daple*$^{+/+}$ mice (Fig. 1B), which is consistent with a previous report regarding neonatal cochleae (Siletti et al., 2017). In addition, we found that the gross shape and size of the cochleae in *Daple*$^{-/-}$ mice were also similar to those of the cochleae in *Daple*$^{+/+}$ mice at 4 weeks of age. These results confirmed that sound wave transmission along the snail-like tube of the OC from the tympanic membrane occurs in the same way in the cochleae of both *Daple*$^{+/+}$ and *Daple*$^{-/-}$ mice [10]. Because the expression of Daple was similar between infants and adults, along the apex to the base, in the cochlea (Fig. 1 C, D; Supplementary Fig. S1), the hearing disturbances observed at all sound frequencies in Daple$^{-/-}$ mice are reasonable, although disruption at higher frequencies suggested the presence of certain functional and/or structural failures involving HCs in the more basal regions of the OC.

Hair bundle arrangement was affected in adult *Daple*$^{-/-}$ mice, especially in the basal region

Based on the abovementioned observations, we next examined the possible links between the ABR results and morphological defects in hair bundles in adult *Daple*$^{-/-}$ mice, aged 8–12 weeks, for the first time, using scanning electron microscopy (SEM). In adult mouse OHCs, deformities were observed in the hair bundles (Fig. 2A), along with various morphological alterations similar to those observed in prior studies on neonatal *Daple*$^{-/-}$ mice[8] ; these were classified as follows: normal (Fig. 2B a, b), flat (Fig. 2B c, d), split (Fig. 2B e, f), and other dysmorphic bundles (Fig. 2B g, h). Although defects in the arrangement of hair bundles were observed over the entire length of the cochlea, the number of cells with defects in hair bundles was higher in the more basal regions of the cochlea in *Daple*$^{-/-}$ mice (% ratios of each dysmorphic bundle type from the apex to the base region, respectively: 17.4, 25.6, 28.8 in flat; 7.8, 24.5, 39.1 in split; 6.5, 7.5, and 17.1, respectively). The abundance of normal hair bundles was decreased in the basal region compared with that in the apex (Fig. 2C). In contrast, in *Daple*$^{+/+}$ mice, almost all the HCs exhibited normal V-shaped bundles (Fig. 2C *Daple*$^{+/+}$; apex 91 cells, middle 95 cells, base 94 cells). The increase in the ratio of abnormal hair bundle arrangement cells from 32% in the apex to 58% in the media to 85% in the base suggested a link between the ABR results and morphological defects in hair bundles in 8–12-week-old adult *Daple*-deficient mice.

Deformed apical structures, comparable to those in 8–12-week-old adult mice, were present in postnatal day (PND)3 *Daple*$^{-/-}$ mice

To compare morphological changes in hair bundles with age, we next focused on the cochleae of infant mice. Various forms of deformities in apical hair bundles

were also detected in PND3 infant *Daple*$^{-/-}$ mice (Fig. 3A). Actin and actin-related proteins were unchanged in these bundles of both the adult and PND3 (Supplementary Fig. S2). As for the kinocilia, they were not always in the center of hair bundles (Fig. 3B). Some kinocilia were located at the center of hair bundles, while the bundles were split (Fig. 3B b). To statistically evaluate apical morphological deformities, we classified kinocilia into three groups based on their localization relative to the hair bundle: normal (centered), off-centered, and poorly determined. The term “poorly examined” was used when the position could not be determined as centered or off-centered (Fig. 3B a). The results showed that >50% of the kinocilia were localized away from the center of the hair bundles, showing a disrupted link between kinocilia and hair bundles (Fig. 3C). In terms of the arrangements of hair bundles, approximately 80% of HCs were abnormal in the basal region of the cochleae, which is the most developmentally mature cochlear region.

Apical microtubules emanate irregularly from disorderly aggregated structures in murine *Daple*$^{-/-}$ cochlear hair cells

Prior studies on ependymal cells have shown that Daple functions as a regulator of polymerization of microtubules in mouse ventricles[7]. In cochlear HCs, apical microtubules are also important regulators of the apical morphogenesis of HCs of the OC. In this study, we focused on the apical microtubule networks of HCs of the OC to clarify their roles in apical morphogenesis in *Daple*$^{-/-}$ mice.

In PND0 *Daple*$^{+/+}$ HCs, apical microtubules were laterally localized, consistent with the lateral positioning of the kinocilium along the mediolateral axis in HCs. The microtubules spread from the pericentriolar region, the base of the kinocilium, toward the cell cortex, to attach to the lateral side of the plasma

membrane (Fig. 4A; *Daple*$^{+/+}$). On the contrary, the opposing ends of microtubules formed ring-like structures around the centrosome. In *Daple*$^{-/-}$ HCs, densely aggregated microtubules in the form of the ring-like structure of microtubules were observed at random positions within the cells, and many microtubules were not attached to the lateral membrane (Fig. 4A). As shown in Fig. 4B in *Daple*$^{+/+}$ HCs, microtubule rings were surrounded by a ring of Daple. The role of Daple in the correct setting of the microtubule network in the apical region is evident from Fig. 4B. The presence of Daple was confirmed by staining *Daple*$^{-/-}$ and *Daple*$^{+/+}$ HCs of the OC with the same antibody.

To examine the 3D structure of the apical microtubule network in detail, we compared the z-series of images for microtubules/EB-1 (Fig. 4C). In *Daple*$^{+/+}$ mice, the laterally deviated microtubule network, the center of which has a halo region, radially and dominantly emanated to the lateral side, whereas smaller amounts of microtubules were diffusely directed to the medial side. The microtubules diffused like an umbrella in *Daple*$^{+/+}$ HC. Upon comparing the distribution of EB-1, a microtubule plus-ended binding protein, to that of microtubule, EB-1 was found to be diffusely distributed through the cytoplasm relatively merged with the distribution of microtubule. In contrast, in murine *Daple*$^{-/-}$ HCs, microtubule plus-ends were aggregated disorderly, without halo regions in the centers of aggregation, and a smaller amount of the microtubule network, diffused within the cytoplasm, was observed compared to that in *Daple*$^{+/+}$ HCs. When z-sliced images were observed, microtubule aggregates were clearly present at very high densities in *Daple*$^{-/-}$ mice. The results are illustrated in Fig. 5A and suggest that Daple plays a role in forming correct microtubule networks in mouse HCs.

Disordered microtubules were observed to run through the HC apical planes in transmission electron microscopy (TEM) images of *Daple*$^{-/-}$ mice

To obtain a clearer distribution of the microtubule network, we next performed thin-section TEM (Fig. 5B). In the thin-section TEM images of *Daple*$^{+/+}$ mice, microtubules surrounding the centrosome were clearly observed, but those around the centrosome seemed relatively sparse, suggesting that this area may be the halo region observed in immunofluorescence images. Microtubules were found to emanate from the pericentriolar region and attached to the lateral cell membrane in HCs. A smaller number of microtubules seemed to run in the medial direction. In contrast, in *Daple*$^{-/-}$ mice, as evident from the immunofluorescence images (Fig. 4), a higher density of microtubules compared with that in cochleae of *Daple*$^{+/+}$ mice was present around the centrosomes without halos, forming a sparse region. Furthermore, some microtubules were unnaturally elongated in the cytoplasm. These results showed that the deficiency in Daple induced disturbed microtubule arrays in mice.

Cochlear hair bundle abnormalities were induced by nocodazole, a microtubule polymerization inhibitor

The abovementioned results suggest that disordered microtubules contribute to the deformity in hair bundles in *Daple*$^{-/-}$ mice. To prove the validity of this hypothesis, we performed nocodazole treatment-based experiments in an organ culture of OC cells (Fig. 6A). The base region of the cochlea from embryonic day (E)17.5 mice was dissected, and the epithelial layer with three arrays of OHCs and one array of IHC was mechanically isolated under a stereo microscope for subsequent organ culture. DMSO-treated samples were prepared for use as a

214 control (Fig. 6B; DMSO). Without nocodazole, almost all HCs developed normally.
215 Upon exposure to nocodazole (400 nM) for 2 days at 37 ° C in a 5% CO_2
216 incubator, stereocilia developed mis-shaped hair bundles, with various kinds of
217 changes, including the presence of flat, dysmorphic, or off-centered kinocilia in
218 HCs, similar to those in *Daple*$^{-/-}$ mice (Fig. 6B, C). Approximately half of the
219 cochlear culture HCs treated with 400 nM nocodazole did not develop correct hair
220 bundles and, instead, had dysmorphic bundle patterns (Fig. 6D). No changes in
221 the expression of PCP core protein were observed under these conditions,
222 suggesting that these results were not related to tissue PCP but to cellular signals
223 (Supplementary Fig. S3).
224

Discussion

Here, first, hearing defects across a broad range of frequencies, especially at frequencies >24 kHz, were found in 8–12-week-old adult *Daple*$^{-/-}$ mice. This result was consistent with the observation that more severe defects in the arrangement of hair bundles were present in more basal areas of the OC, as detected by SEM imaging. By comparing adult and infant mice (around PND3), we also found that defects did not clearly progress in the apical structure of hair cells after the neonatal stage. This suggested consistent roles of Daple after maturation of apical structures of HCs in the OC. Daple exhibited regulation of the microtubule network in HCs around the neonatal stage. To identify the apical microtubule network as a critical regulator of apical deformities in the HCs of the OC in *Daple*$^{-/-}$ mice, we performed immunofluorescence staining, scanning, TEM, and organ culture of OC cells with/without nocodazole treatment.

In ventricular ependymal cells, Daple is reported to function in microtubule dynamics. In previous reports, microtubules were suggested to be important for the apical arrangement of HCs[9]. Several microtubule-related proteins, such as Lis1, a dynein activating microtubule-binding protein, the conditional knockout of which disturbs the organization of microtubules by impairing developmental stage-specific connections between the microtubules and plasma membranes through the LGN (Gpsm2)–Gαi–dynein complex[9]. This might lead to the formation of an apical microtubule-rich bare zone and the stabilization of Gαi3–Daple–Dvl complexes on the abneural side of the plasma membrane in HCs. Our results regarding the dysregulation of EB1 and focal localization in *Daple*$^{-/-}$ mice also support this notion. On the contrary, Dvl, a binding partner of Daple, is also indispensable for apical morphogenesis. Dvl deficiency induces various degrees of malformation of hair bundles because of defects in the combination of Dvl 1–

3, as reported previously[11] [12]. In this sense, a close relationship between microtubules and apical structures, including stereocilia/kinocilia morphogenesis, is suggested.

Because sounds with a frequency >24 kHz can cause approximately 30% of the basal region of the membrane to vibrate, our ABR results are assumed to reflect the severity of deformities of basal stereocila bundles in adult *Daple*$^{-/-}$ mice. The mechanism by which the basal region of the OC in *Daple*$^{-/-}$ mice was more severely deformed is unknown. There was a recent report concerning the special role of Gαi$_3$ activation through the GBA domain[13], and mislocalization of apical Gαi$_3$ in HCs in Daple-deficient mice[8]. Gαi$_3$ mutant mice exhibited more severe mis-shaped hair bundle arrangements in the basal area of the cochlea duct[14]. This led us to imagine the presence of some correlation between Daple deficiency and Gαi$_3$ function, specifically in the basal region of the OC. Additionally, Dvl subtype-specific interactions with Daple may induce severe basal changes in Daple-deficient mice.

The shape and size of the cochlear ducts in *Daple*$^{-/-}$ mice were comparable to those of cochlear ducts in both PND0 and 4-weeks-old *Daple*$^{+/+}$ mice. Several reports have demonstrated that other PCP pathways and dysfunction of the actin cytoskeleton involve various forms of cochlear malformation. PCP proteins, such as Vangl, have a normal V-shape, but disorientated, hair bundle arrangements that are different from those in *Daple*$^{-/-}$ mice[15]. As for actin, it is informative to investigate Rho-family protein-deficient mice, because of the upstream regulatory role of Rho-family proteins in the organization of actin filaments. Rac1-deficient mice have defects in the arrangement of hair bundles similar to those in Daple-deficient mice, but these are different from those in *Daple*$^{-/-}$ mice in that the cochlear duct is shortened and the fragmentation of hair bundles is severely

277 progressive around birth[16]. Moreover, the cochlear abnormalities observed in
278 *Daple*$^{-/-}$ mice were different from those in mice deficient in actomyosin-related
279 proteins, such as myosin2[17], RhoA[18], and Cdc42[19 20].

280 We validated the hypothesis that Daple regulates the organization of
281 microtubules in HCs of the OC, in addition to that in ependymal cells. E17.5
282 mouse cochlear organ culture showed that the defects in the arrangements of
283 stereocilia bundles after treatment with nocodazole were similar to those in
284 Daple-deficient mice. This is the first study regarding HC differentiation in the
285 cochlea employing microtubule polymerization inhibitors, except for the
286 examination of apical surface rigidity[21]. Further studies examining cochlear
287 cytoskeletal maturation processes in shorter intervals around birth may reveal the
288 sequence of underlying molecular mechanisms and their related signals.
289

Methods

All methods were conducted in accordance with ARRIVE guidelines.

Ethics Statement.

Animal experiments were performed in accordance with protocols approved by the animal studies committee of Osaka University, School of Medicine and Frontier Biosciences. Recombinant DNA experiments were carried out in accordance with the protocols approved by Osaka University.

Generation of Daple-Deficient Mice.

We used a targeted ESC clone (DEPD00564-1-G07) from the trans-NIH KOMP Repository (University of California, Davis) to generate Daple mutant mice as previously reported [7]. Animal care and use was in accordance with the Guidelines for Proper Conduct of Animal Experiments in Osaka University and was approved by the Animal Care and Use Committee at Osaka University.

Auditory Brainstem Response (ABR) Test.

The details of the ABR test and the method have been reported previously [22]. We injected ketamine (100 mg/kg) and xylazine (10 mg/kg) into the peritoneal cavity of mice and put mice into a sound isolation chamber. Subcutaneous needle electrodes were inserted in the pinna and vertex, with a ground electrode near the tail. Responses to tone pip stimuli were recorded at 4, 8, 12, 24, and 32 kHz in 8–10-week-old mice using a Power Lab 2/25 (AD Instruments, Australia) and a TDT Auditory Workstation (Tucker-Davis Technologies, Alachua, Florida, USA). The duration of tone bursts was 1 ms. We amplified and averaged 500 responses. All ABRs were measured without knowing the mice profiles or genotypes.

Assessment of Daple gene expression by X-gal staining.

Inner ears obtained from Daple +/- and Daple+/+ adult mice were fixed in 4% paraformaldehyde (PFA) in PBS for 15–30 min. Staining was performed for 48 h at 37 °C in 2 mg/mL X-gal (Promega) in PBS/2 mM $MgCl_2$/0.02% NP40/0.01% sodiumdeoxycholate/5 mM $K_4Fe(CN)_6$/5 mM $K_3Fe(CN)_6$.

Immunofluorescence staining.

Inner ears obtained from Daple+/+ or Daple-/-mice were dissected from adult mice or pups and fixed in 4% PFA in PBS at 4 °C overnight, or in absolute methanol at -20 °C for 10–20 min, or in 10% TCA on ice for 1 h. After fixation in 4% PFA or absolute methanol, adult inner ears were decalcified in EDTA. After fixation of the inner ears by PFA, they were permeabilized with 0.15% Triton X-100 in PBS at room temperature (RT) for 15 min. Whole mount organs were blocked for 1 h with 10% bovine serum albumin in PBS or with the blocking reagent (M.O.M.™; Vector Laboratories, Inc.). They were incubated with primary antibodies and washed three times with PBS. Staining was performed with Alexa Fluor-conjugated secondary antibodies at RT for 1 h. The following primary antibodies were used: monoclonal anti-mouse α-tubulin antibody (T9026; Sigma-Aldrich) 1:500; anti-rabbit Daple antibody (28147; IBL) 1:100; anti-rat ZO-1 antibody (PA5-18646; Thermo fisher) 1:400; anti-rat tyrosinated alpha-tubulin (ab6160; Abcam) 1:500; anti-mouse EB-1 (610535; BD) 1:500; anti-goat Frizzled 6 (AF1526; R&D Systems) 1:200; anti-rabbit myosin2A (M8064; Sigma-Aldrich) 1:200; and anti-rabbit Par-3 (07–330; Sigma-Aldrich) 1:500. The following secondary antibodies were used: Alexa Fluor 488-conjugated donkey anti-mouse IgG (Jackson Immuno Research) 1:500; Cy3-

conjugated donkey anti-rat IgG, Alexa Fluor 647-conjugated donkey anti-rabbit IgG; Alexa Fluor 647-conjugated donkey anti goat IgG; and rhodamine phalloidin (Cytoskeleton, Inc.) 1:500. Images were collected using a Zeiss LSM 710 or LSM 880 confocal microscope, and the obtained images were analyzed with the Zen Software.

Scanning electron microscopy (SEM).

Inner ears obtained from Daple +/+ or Daple-/- mice were fixed with 2% PFA and 2.5% glutaraldehyde in 0.1 M HEPES (pH 7.4) for 1 h at RT. They were then washed with 0.1 M HEPES and fixed in 1% OsO4 for 1 h on ice, incubated in 1% tannic acid overnight, and fixed with 1% OsO4 for 1 h on ice. The organ of Corti was micro-dissected, dehydrated, dried at the critical point, sputter-coated, and observed by SEM (S-4800 microscope; Hitachi).

Transmission electron microscopy (TEM).

Inner ears obtained from Daple +/+ or Daple-/- mice were fixed with 2% PFA and 2.5% glutaraldehyde and treated with 2% tannic acid in 0.1 M HEPES (pH 7.4) for 1 h at RT. They were then washed with 0.1 M HEPES and fixed in 1% OsO4 for 2 h on ice. The organ of Corti was micro-dissected, dehydrated, embedded, sectioned, and observed by TEM (JEM-1400Plus; JEOL).

Culture of embryonic mouse cochlea and drug treatment.

Cochlear organ culture was started from E17.5 mice. Briefly, cochleae were dissected in Leibobitz L-15 medium (Thermo Fisher Scientific) and established on coverslips coated with Matrigel matrix (Corning). Explants were then maintained for 1 h in vitro in DMEM/F-12 (Invitrogen) supplemented with FBS

and ampicillin (Nacalai Tesque). Next, the medium was replaced with that containing DMSO only (control) or nocodazole (Sigma; 400 and 800 nM). After 2 days of culture in vitro, the explants were fixed with 4% PFA or methanol for immunostaining, or with 2% PFA plus 2.5% glutaraldehyde in 0.1 M HEPES (pH 7.4) for SEM.

Statistical analysis.

All data are expressed as mean ± SEM. Comparisons between two groups were performed using Student's *t*-test, and differences with $P < 0.05$ were considered statistically significant.

References

1 Butler, M. T. & Wallingford, J. B. Planar cell polarity in development and disease. *Nat Rev Mol Cell Biol* **18**, 375-388, doi:10.1038/nrm.2017.11 (2017).

2 Munnamalai, V. & Fekete, D. M. Wnt signaling during cochlear development. *Semin Cell Dev Biol* **24**, 480-489, doi:10.1016/j.semcdb.2013.03.008 (2013).

3 Oshita, A. *et al.* Identification and characterization of a novel Dvl-binding protein that suppresses Wnt signalling pathway. *Genes cells* **8**, 1005-1017, doi:10.1046/j.1365-2443.2003.00692.x (2003).

4 Aznar, N. *et al.* Daple is a novel non-receptor GEF required for trimeric G protein activation in Wnt signaling. *Elife* **4**, e07091, doi:10.7554/eLife.07091 (2015).

5 Drielsma, A. *et al.* Two novel CCDC88C mutations confirm the role of DAPLE in autosomal recessive congenital hydrocephalus. *J Med Genet* **49**, 708-712, doi:10.1136/jmedgenet-2012-101190 (2012).

6 Ekici, A. B. *et al.* Disturbed Wnt Signalling due to a Mutation in CCDC88C Causes an Autosomal Recessive Non-Syndromic Hydrocephalus with Medial Diverticulum. *Mol Syndromol* **1**, 99-112, doi:10.1159/000319859 (2010).

7 Takagishi, M. *et al.* Daple Coordinates Planar Polarized Microtubule Dynamics in Ependymal Cells and Contributes to Hydrocephalus. *Cell Rep* **20**, 960-972, doi:10.1016/j.celrep.2017.06.089 (2017).

8 Siletti, K., Tarchini, B. & Hudspeth, A. J. Daple coordinates organ-wide and cell-intrinsic polarity to pattern inner-ear hair bundles. *Proc Natl Acad Sci U S A* **114**, E11170-E11179, doi:10.1073/pnas.1716522115. (2017).

9 Sipe, C. W., Liu, L., Lee, J., Grimsley-Myers, C. & Lu, X. Lis1 mediates planar polarity of auditory hair cells through regulation of microtubule organization. *Development* **140**, 1785-1795, doi:10.1242/dev.089763 (2013).

10 Muller, M., von Hunerbein, K., Hoidis, S. & Smolders, J. W. A physiological place-frequency map of the cochlea in the CBA/J mouse. *Hear Res* **202**, 63-73, doi:10.1016/j.heares.2004.08.011 (2005).

11 Etheridge, S. L. *et al.* Murine dishevelled 3 functions in redundant pathways with dishevelled 1 and 2 in normal cardiac outflow tract, cochlea, and neural tube development. *PLoS Genet* **4**, e1000259, doi:10.1371/journal.pgen.1000259 (2008).

12 Wang, J. *et al.* Dishevelled genes mediate a conserved mammalian PCP pathway to regulate convergent extension during neurulation. *Development* **133**, 1767-1778, doi:10.1242/dev.02347 (2006).

13 Marivin, A. *et al.* GPCR-independent activation of G proteins promotes apical cell constriction in vivo. *J Cell Biol* **218**, 1743-1763, doi:10.1083/jcb.201811174 (2019).

14 Beer-Hammer, S. *et al.* Galphai Proteins are Indispensable for Hearing. *Cell Physiol Biochem* **47**, 1509-1532, doi:10.1159/000490867 (2018).

15 Copley, C. O., Duncan, J. S., Liu, C., Cheng, H. & Deans, M. R. Postnatal refinement of

auditory hair cell planar polarity deficits occurs in the absence of Vangl2. *J Neurosci* **33**, 14001-14016, doi:10.1523/JNEUROSCI.1307-13.2013 (2013).

16 Grimsley-Myers, C. M., Sipe, C. W., Geleoc, G. S. & Lu, X. The small GTPase Rac1 regulates auditory hair cell morphogenesis. *J Neurosci* **29**, 15859-15869, doi:10.1523/JNEUROSCI.3998-09.2009 (2009).

17 Yamamoto, N., Okano, T., Ma, X., Adelstein, R. S. & Kelley, M. W. Myosin II regulates extension, growth and patterning in the mammalian cochlear duct. *Development* **136**, 1977-1986, doi:10.1242/dev.030718 (2009).

18 Sai, X., Yonemura, S. & Ladher, R. K. Junctionally restricted RhoA activity is necessary for apical constriction during phase 2 inner ear placode invagination. *Dev Biol* **394**, 206-216, doi:10.1016/j.ydbio.2014.08.022 (2014).

19 Kirjavainen, A., Laos, M., Anttonen, T. & Pirvola, U. The Rho GTPase Cdc42 regulates hair cell planar polarity and cellular patterning in the developing cochlea. *Biol Open* **4**, 516-526, doi:10.1242/bio.20149753 (2015).

20 Ueyama, T. *et al.* Maintenance of stereocilia and apical junctional complexes by Cdc42 in cochlear hair cells. *J Cell Sci* **127**, 2040-2052, doi:10.1242/jcs.143602 (2014).

21 Szarama, K. B., Gavara, N., Petralia, R. S., Kelley, M. W. & Chadwick, R. S. Cytoskeletal changes in actin and microtubules underlie the developing surface mechanical properties of sensory and supporting cells in the mouse cochlea. *Development* **139**, 2187-2197, doi:10.1242/dev.073734 (2012).

22 Hanada, Y. *et al.* Epiphycan is specifically expressed in cochlear supporting cells and is necessary for normal hearing. *Biochem Biophys Res Commun* **492**, 379-385, doi:10.1016/j.bbrc.2017.08.092 (2017).

Acknowledgements

We thank the laboratory members for helpful discussions. We also thank Professor Shoichi Shimada, Department of Neuroscience and Cell Biology, Graduate School of Medicine, Osaka University, for the expert advice and Mr. Eiji Oiki, Center for Medical Research and Education, Graduate School of Medicine, Osaka University, for the technical advice. This work was supported by Grants-in-Aid for Early-Career Scientists Grant Number JP18K16887 (to Y.O.), the Japan Science and Technology Core Research for Evolutionary Science and Technology Agency CREST (to S.T.), Grant-in-Aid for Scientific Research of Innovative Areas from the Ministry of Education, Culture, Sports, and Technology (MEXT) (to S.T.) of Japan, and Grant-in-Aid for Scientific Research (A) (to S.T.) and (B) (to A.T.).

Author Contributions Statement

Y.O., S.N., Y.H., and K.O. performed the experiments; Y.O., S.N., E.H., Y.H., K.O., M.T., M.T., T.I., Y.O., K.O., T.S., H.I., and S.T. shared reagents, help, and advice; Y.O., A.T., and S.T. designed the research, analyzed the data, and wrote the manuscript.

Additional information

Declaration of Interests

The authors declare no competing interests.

467

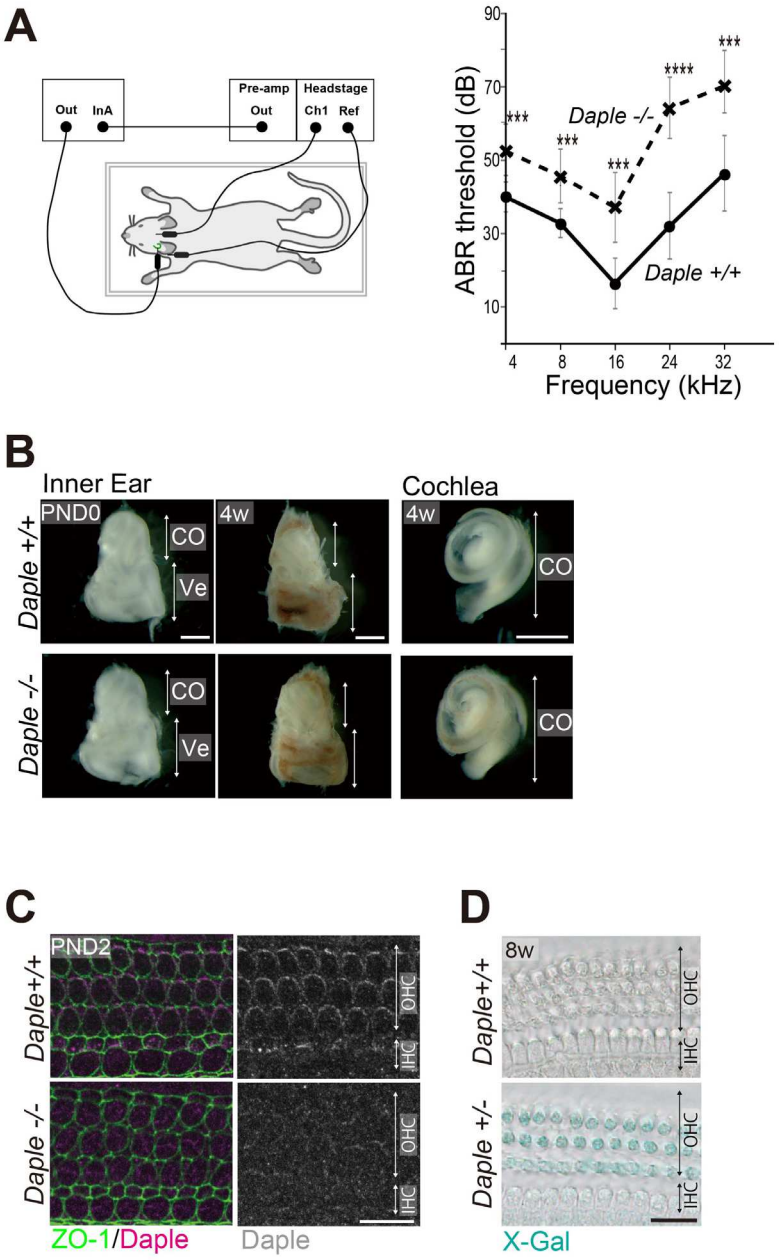

Figure 1. **Hearing ability, inner ear morphology, and Daple expression in Daple-deficient mice**

(A) The auditory brainstem response (ABR) thresholds of *Daple*$^{-/-}$ mice (8–12-weeks-old, n = 7) were significantly higher below a 24 kHz frequency stimulus than those of *Daple*$^{+/+}$ mice (8–12-weeks-old, n = 7; $p < 0.001$). At around 24 kHz, ABR thresholds were significantly higher than in control mice ($p < 0.0001$). ***$p < 0.001$, ****$p < 0.0001$. (B) The gross observation and length of the cochlear duct

476 in the inner ears of *Daple*$^{+/+}$ and *Daple*$^{-/-}$ mice (postnatal day (PND)0, 4-weeks-
477 old) seemed normal. (C) Immunostaining of the OC in wild-type PND3 HCs.
478 Daple was stained on the lateral side of OHCs and IHCs. Additionally, some
479 staining of centrioles was evident in HCs. The enrichment was not visible in
480 *Daple*$^{-/-}$ littermates. HC, hair cell; OHC, outer hair cell; IHC, inner hair cell. (D)
481 LacZ-Xgal staining showing expression patterns of *Daple* in adult *Daple*$^{+/-}$ and
482 *Daple*$^{+/+}$ cochleae. *Daple*$^{+/-}$ OHCs are stained blue. Scale bars: B; 1 mm, C; 10
483 μm, D; 20 μm.
484

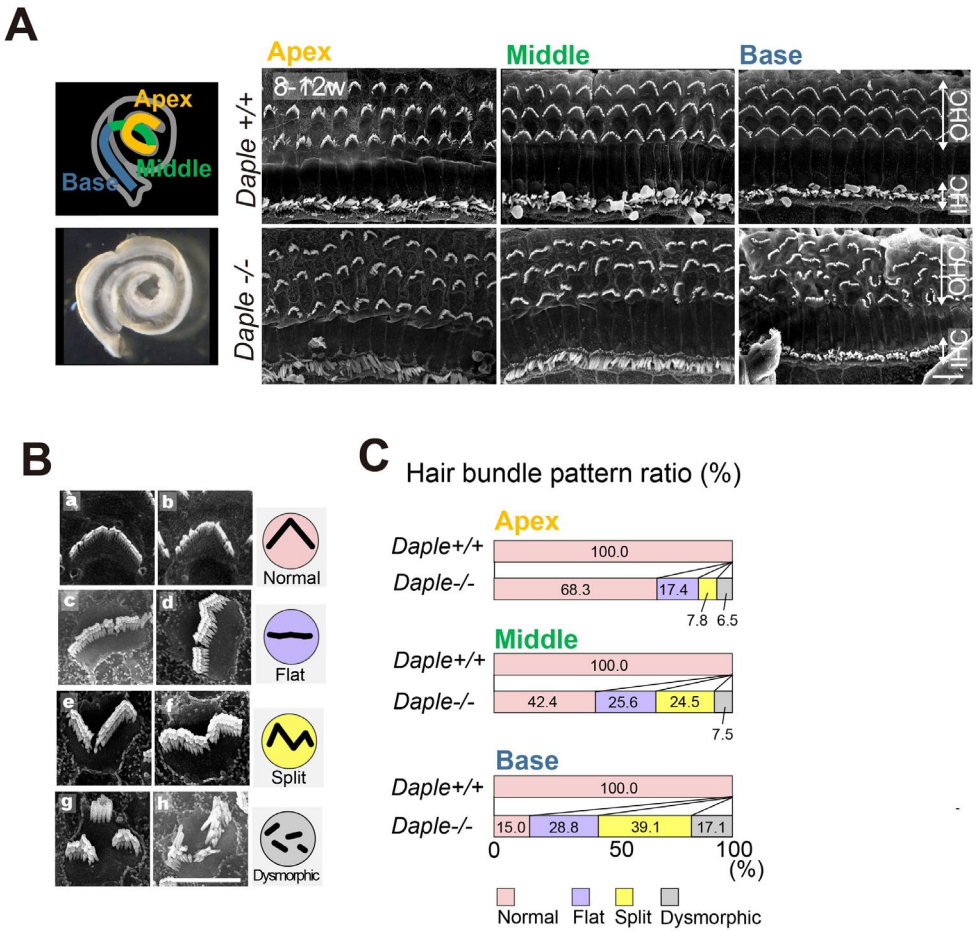

485

486 **Figure 2. Scanning electron microscopy (SEM) analysis of Daple-deficient**

487 **organ of Corti (OC) in adult mice**

488 (A) SEM images of hair cells (HCs) from apical, middle, and basal areas of

489 *Daple*$^{+/+}$ and *Daple*$^{-/-}$ cochleae in adult mice. *Daple*$^{-/-}$ cochleae exhibit major

490 anomalies in hair bundles in OHCs, high magnification images of OHCs. *Daple*$^{-/-}$

491 HCs with flat bundles (jagged horizontal line). (B a, b) *Daple*$^{-/-}$ HCs with split

492 bundles (reversed apex region of the V-shape bundle). (B c, d) *Daple*$^{-/-}$ HCs with

493 a generally deformed bundle (dysmorphic bundle; fragmented bundle) (B e, f).

494 Scale bars: A; 10 μm, B–G; 5 μm. (C) Analysis of the difference between

495 Daple+/+ and *Daple*-/- mice in the three cochlear areas (apex, middle, and basal

496 areas), (8–12-weeks-old, Daple +/+ apex 91 cells, middle 95 cells, and basal 94

cells, *Daple*$^{-/-}$ apex 632 cells, middle 477 cells, and basal 455 cells). The ratios of Daple-deficient mouse HCs tended to increase with some deformed bundles.

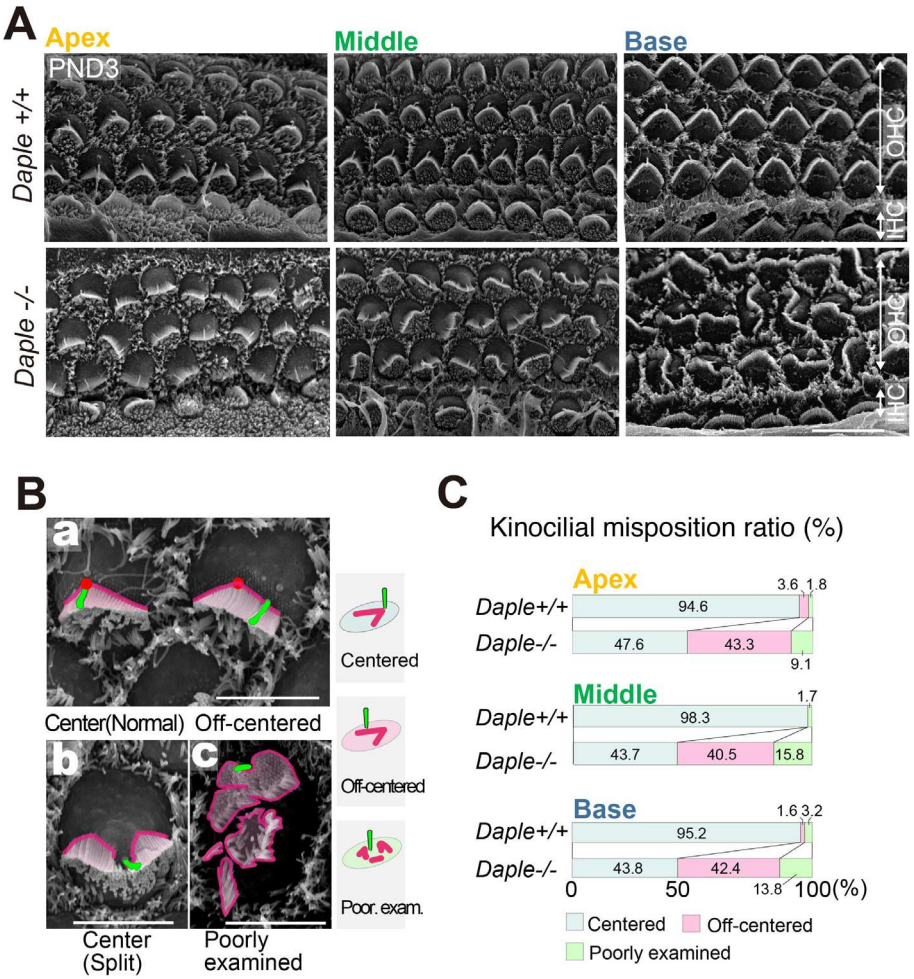

Figure 3. **Analysis of Daple-deficient organ of Corti (OC) in mouse pups**

(A) Scanning electron microscopy images of hair cells (HCs) from the apex, middle, and basal areas of *Daple*$^{+/+}$ and *Daple*$^{-/-}$ cochleae in postnatal day (PND)3 mice. The most severe effects of Daple deficiency were observed in the basal areas of cochlea (Ba). Normal V-shaped bundles and flat bundles in *Daple*$^{-/-}$ mice: arrows show normal kinocilium locations and arrow heads show abnormal kinocilium locations. (Bb) Split and (Bc) dysmorphic bundles: the stepwise arrangement of stereocilia bundles was missing. (C) We classified the localization of kinocilia against hair bundles into three groups: normal (centered), off-centered, and poorly examined. When we could not define the kinocilia, we classified them into the poorly examined group. A significant difference between the normal and

512 off-centered groups was not identified in these observations (at PND3, n = 5;
513 apex 691 cells, middle 886 cells, basal 765 cells). (D) Approximately 80% of HCs
514 were defective in the arrangement of hair bundles in the basal regions of cochlea.
515 Scale bars: (A); 10 μm, (B)–(D); 5 μm.
516

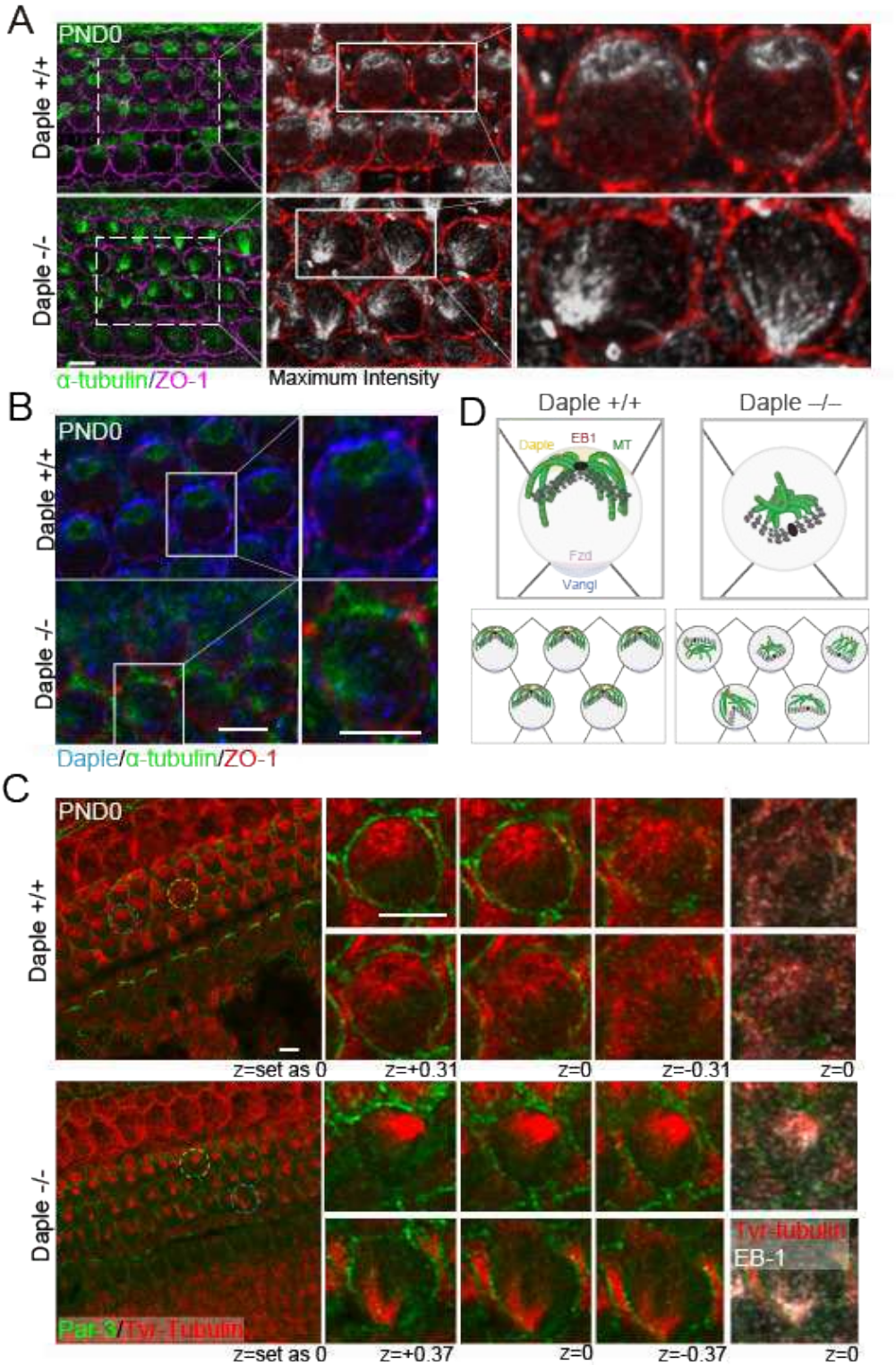

Figure 4. **Microtubules and related protein expression in hair cells (HCs) of the organ of Corti (OC) in *Daple*$^{-/-}$ mice**

(A) Microtubules were spread from the pericentriolar area to outer hair cell (OHC) cortexes, mainly in lateral areas in *Daple*$^{+/+}$ postnatal day (PND)0 mice. The

522 microtubules were disorganized or aggregated around pericentriolar areas in
523 *Daple*$^{-/-}$ PND0 mice. (B) Expression of Daple and microtubule distribution in
524 *Daple*$^{+/+}$ PND0 mice. Daple surrounded the microtubules in the centrosomes of
525 the HCs of *Daple*$^{+/+}$ mice. Some non-specific staining was observed, but ring-like
526 staining was not detected in *Daple*$^{-/-}$ HCs. (C) We compared a z-series of images
527 against microtubules/EB-1. EB-1 was concentrated in microtubule aggregations
528 in many *Daple*$^{-/-}$ HCs. (D) Schematic of apical microtubule networks in HCs of
529 Daple WT mice compared to those of Daple KO mice. Scale bars: A, B, C, 5 μm.
530

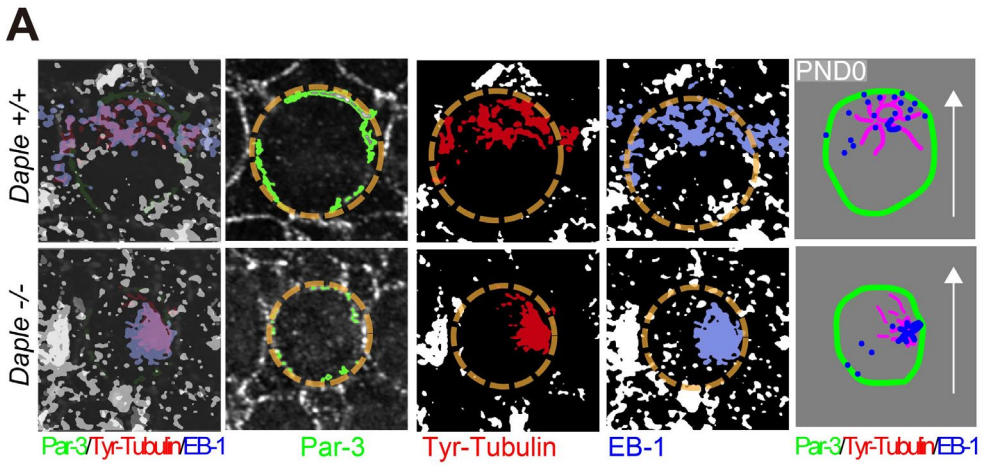

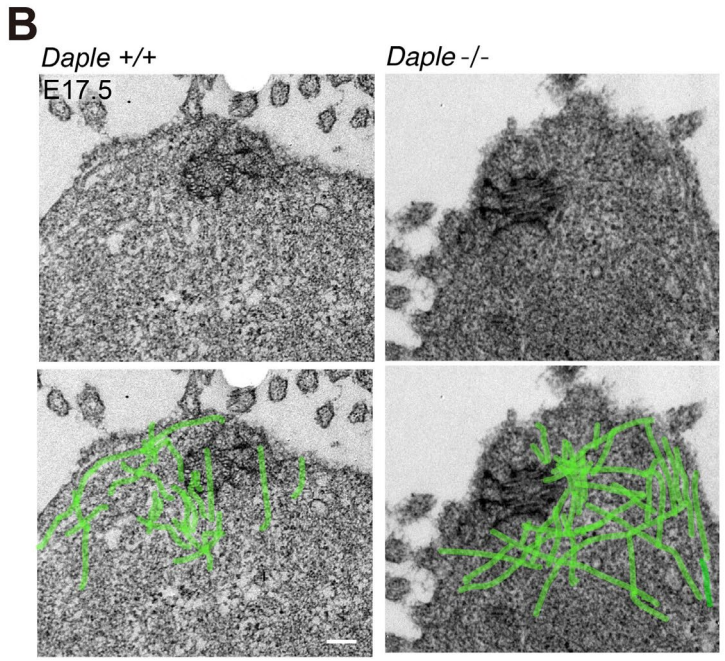

Figure 5. **EB-1/Tyr-tubulin staining and transmission electron microscopy (TEM) images**

(A) Images of EB-1/Tyr-tubulin staining from Figure.4C processed using PhotoShop. The distribution of EB-1, a microtubule plus-end binding protein, was observed near the lateral membrane of hair cells (HCs) in *Daple*$^{+/+}$ mice; however, EB-1 in *Daple*$^{-/-}$ HCs was more densely aggregated in the cytoplasm. (B) The microtubular network extending from the basal body was clearly obsserved in murine *Daple*$^{+/+}$ HCs. However, the microtubules showed a higer dense distribution around basal bodies in *Daple*$^{-/-}$mice. Scale bar: 1 μm.

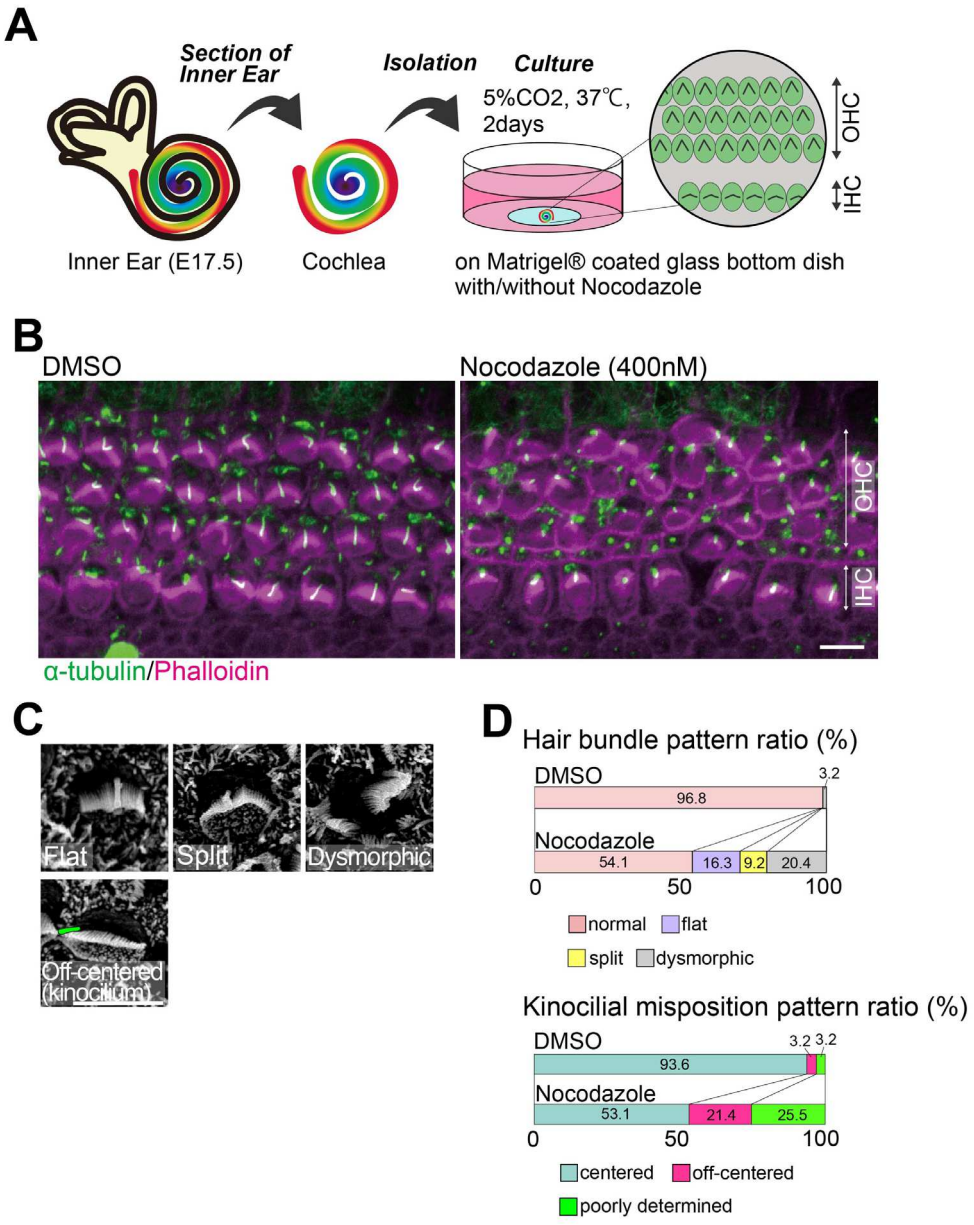

541

542 **Figure 6. Cochlear organ culture with nocodazole treatment**

543 (A) We performed embryonic day (E)17.5 mouse cochlear organ culture. (B) After
544 treatment with 0.05% DMSO or 400 nM nocodazole for 2 days, we performed
545 immunostaining analyses against α-tubulin (green) and phalloidin (magenta).
546 Many stereocilia bundles showed dysmorphic patterns. (C) In scanning electron
547 microscopy (SEM) images, some stereocilia showed mis-shaped and off-
548 centered patterns after nocodazole treatment. (D) To understand any statistical

549 differences between the two groups (cochlear organ culture started at E17.5,
550 DMSO 80 cells, 400 nM nocodazole 98 cells), we counted and summarized them
551 in (D).
552
553

554

Figures

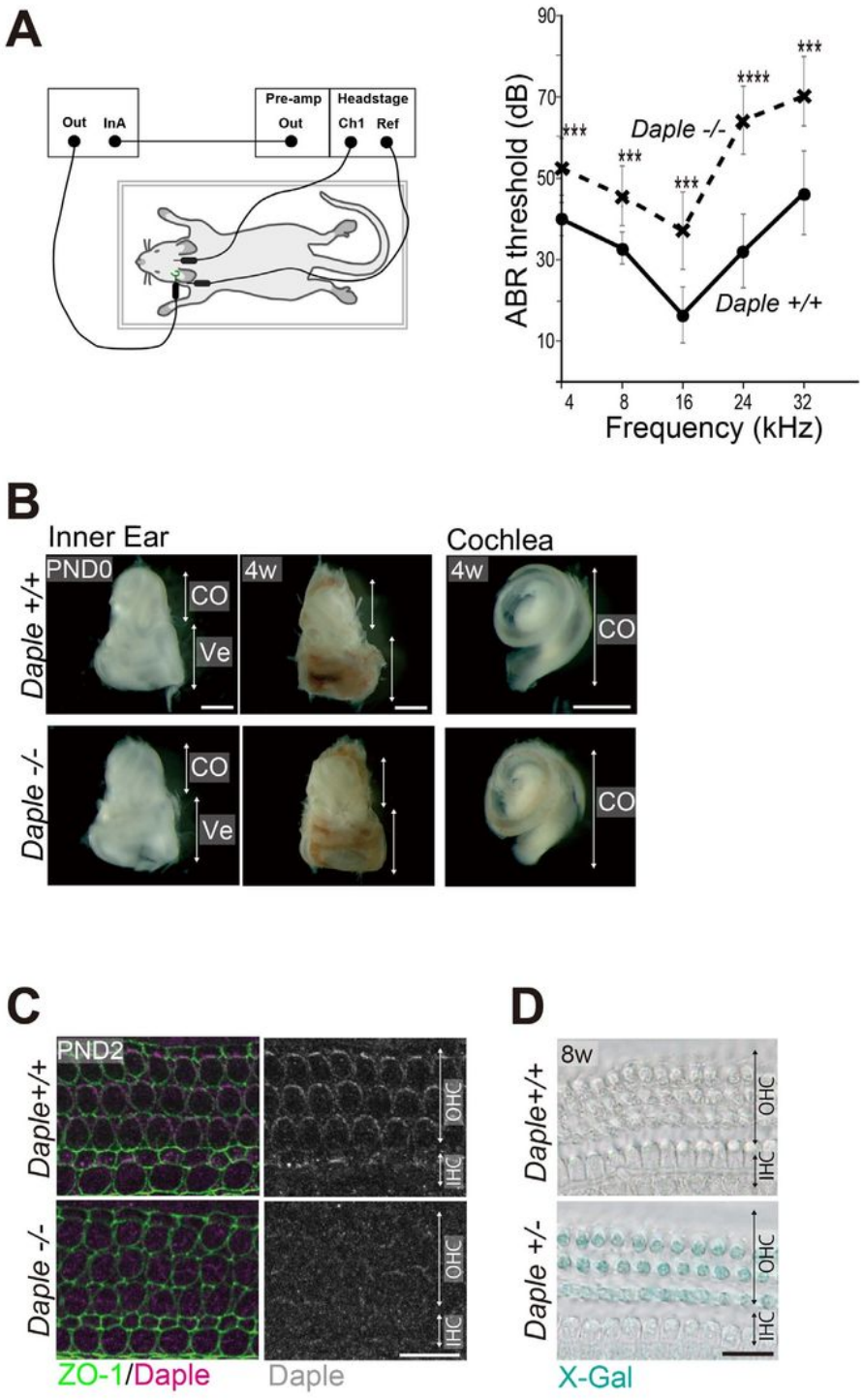

Figure 1

Hearing ability, inner ear morphology, and Daple expression in 469 Daple-deficient mice (A) The auditory brainstem response (ABR) thresholds of Daple-/- mice (8–12- weeks-old, n = 7) were significantly higher below a 24 kHz frequency stimulus than those of Daple+/+ mice (8–12-weeks-old, n = 7; $p < 0.001$). At

around 24 kHz, 473 ABR thresholds were significantly higher than in control mice ($p < 0.0001$). ***$p < 0.001$, ****$p < 0.0001$. (B) The gross observation and length of the cochlear duct in the inner ears of Daple+/+ and Daple-/- mice (postnatal day (PND)0, 4-weeks-476 old) seemed normal. (C) Immunostaining of the OC in wild-type PND3 HCs. Daple was stained on the lateral side of OHCs and IHCs. Additionally, some staining of centrioles was evident in HCs. The enrichment was not visible in Daple-/- littermates. HC, hair cell; OHC, outer hair cell; IHC, inner hair cell. (D) LacZ-Xgal staining showing expression patterns of Daple in adult Daple+/- and Daple+/+ cochleae. Daple+/- OHCs are stained blue. Scale bars: B; 1 mm, C; 10 482 μm, D; 20 μm.

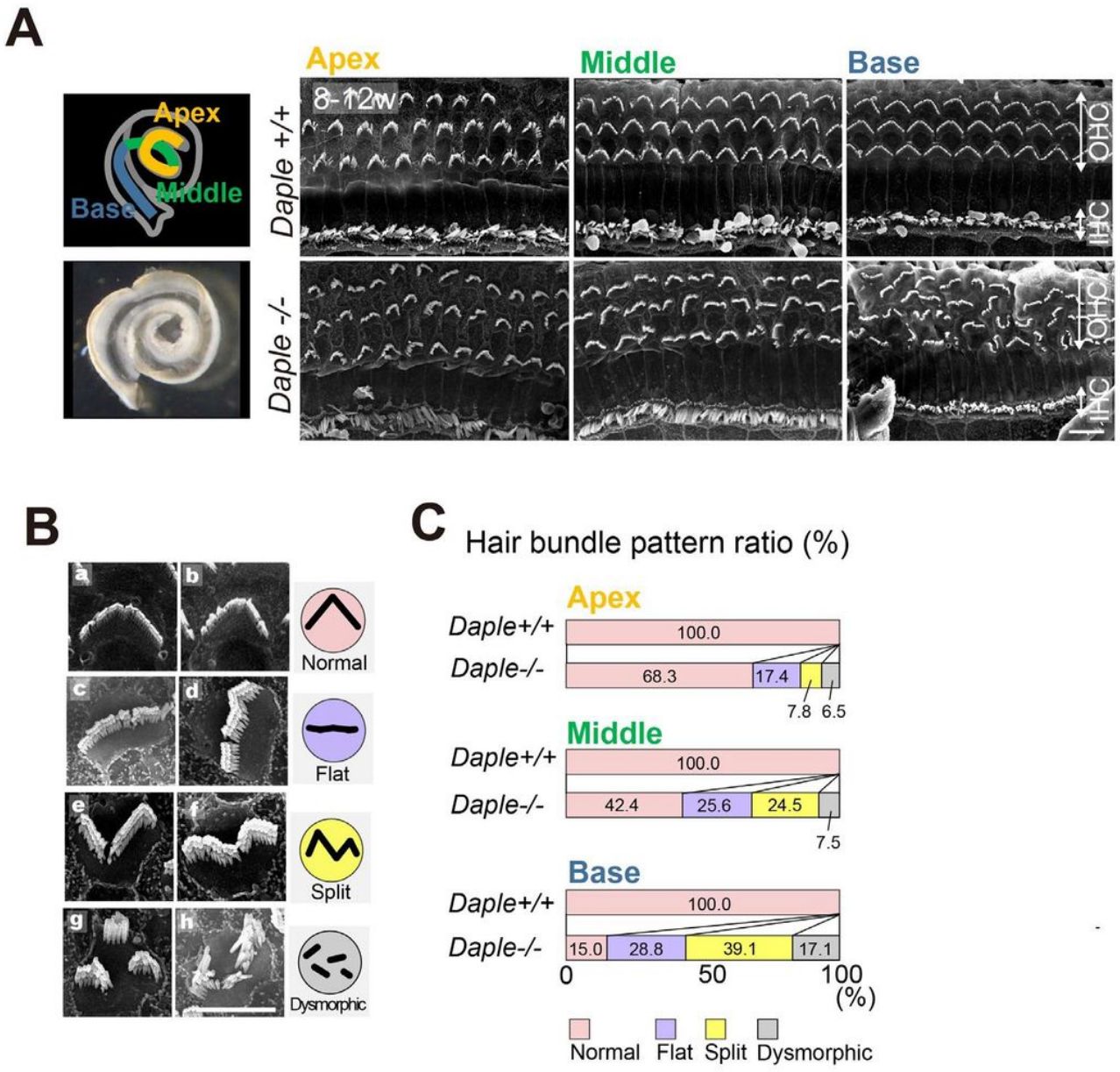

Figure 2

Scanning electron microscopy (SEM) analysis of Daple-deficient organ of Corti (OC) in adult mice (A) SEM images of hair cells (HCs) from apical, middle, and basal areas of Daple+/+ and Daple-/- cochleae

in adult mice. Daple-/- cochleae exhibit major anomalies in hair bundles in OHCs, high magnification images of OHCs. Daple-/- HCs with flat bundles (jagged horizontal line). (B a, b) Daple-/- HCs with split bundles (reversed apex region of the V-shape bundle). (B c, d) Daple-/- HCs with a generally deformed bundle (dysmorphic bundle; fragmented bundle) (B e, f). Scale bars: A; 10 μm, B–G; 5 μm. (C) Analysis of the difference between Daple+/+ and Daple-/- mice in the three cochlear areas (apex, middle, and basal areas), (8–12-weeks-old, Daple +/+ apex 91 cells, middle 95 cells, and basal 94 cells, Daple-/- apex 632 cells, middle cells, and basal 455 cells). The ratios of Daple-deficient mouse HCs tended to increase with some deformed bundles.

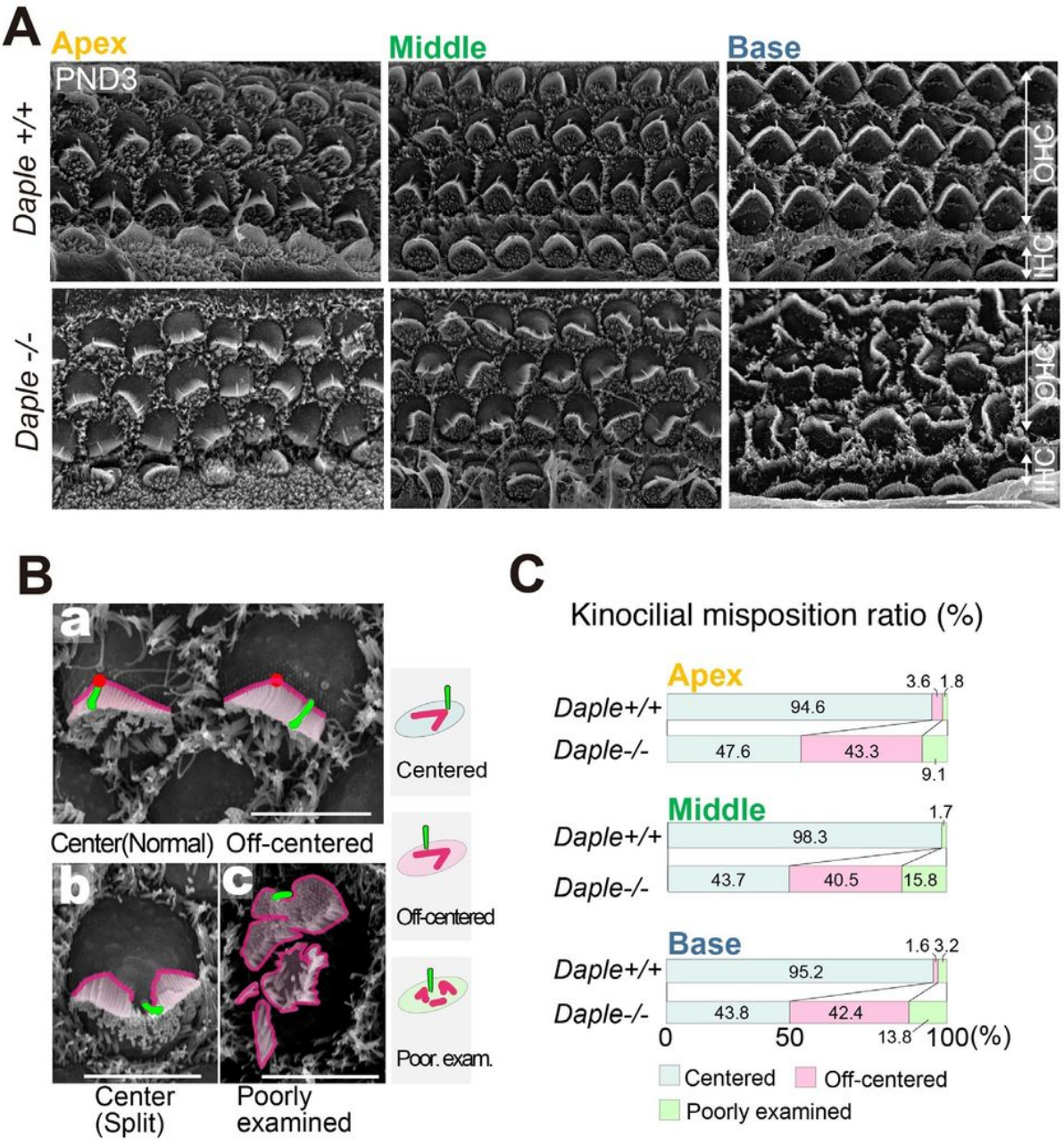

Figure 3

Analysis of Daple-deficient organ of Corti (OC) in mouse pups (A) Scanning electron microscopy images of hair cells (HCs) from the apex,middle, and basal areas of Daple+/+ and Daple-/- cochleae in postnatal day (PND)3 mice. The most severe effects of Daple deficiency were observed in the basal areas of cochlea (Ba). Normal V-shaped bundles and flat bundles in Daple-/- mice: arrows show normal kinocilium locations and arrow heads show abnormal kinocilium locations. (Bb) Split and (Bc) dysmorphic bundles: the stepwise arrangement of stereocilia bundles was missing. (C) We classified the localization of kinocilia against hair bundles into three groups: normal (centered), off-centered, and poorly examined. When we could not define the kinocilia, we classified them into the poorly examined group. A significant difference between the normal and off-centered groups was not identified in these observations (at PND3, n = 5; 512 apex 691 cells, middle 886 cells, basal 765 cells). (D) Approximately 80% of HCs were defective in the arrangement of hair bundles in the basal regions of cochlea. Scale bars: (A); 10 μm, (B)–(D); 5 μm.

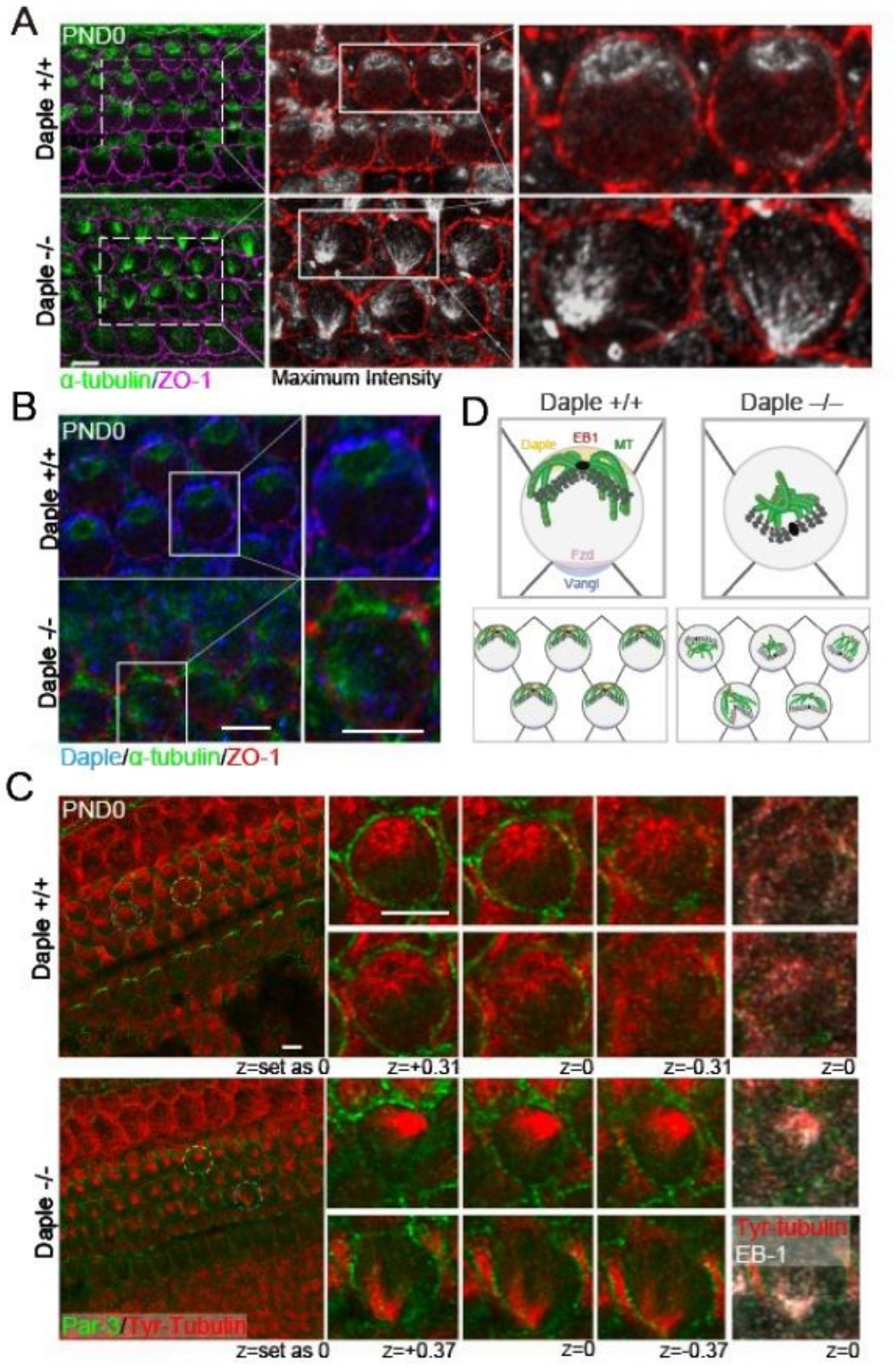

Figure 4

Microtubules and related protein expression in hair cells (HCs) of the organ of Corti (OC) in Daple-/- mice (A) Microtubules were spread from the pericentriolar area to outer hair cell (OHC) cortexes, mainly in lateral areas in Daple+/+ postnatal day (PND)0 mice. The microtubules were disorganized or aggregated around pericentriolar areas in Daple-/- PND0 mice. (B) Expression of Daple and microtubule distribution in Daple+/+ PND0 mice. Daple surrounded the microtubules in the centrosomes of the HCs of Daple+/+

mice. Some non-specific staining was observed, but ring-like staining was not detected in Daple-/- HCs. (C) We compared a z-series of images against microtubules/EB-1. EB-1 was concentrated in microtubule aggregations in many Daple-/- HCs. (D) Schematic of apical microtubule networks in HCs of Daple WT mice compared to those of Daple KO mice. Scale bars: A, B, C, 5 μm.

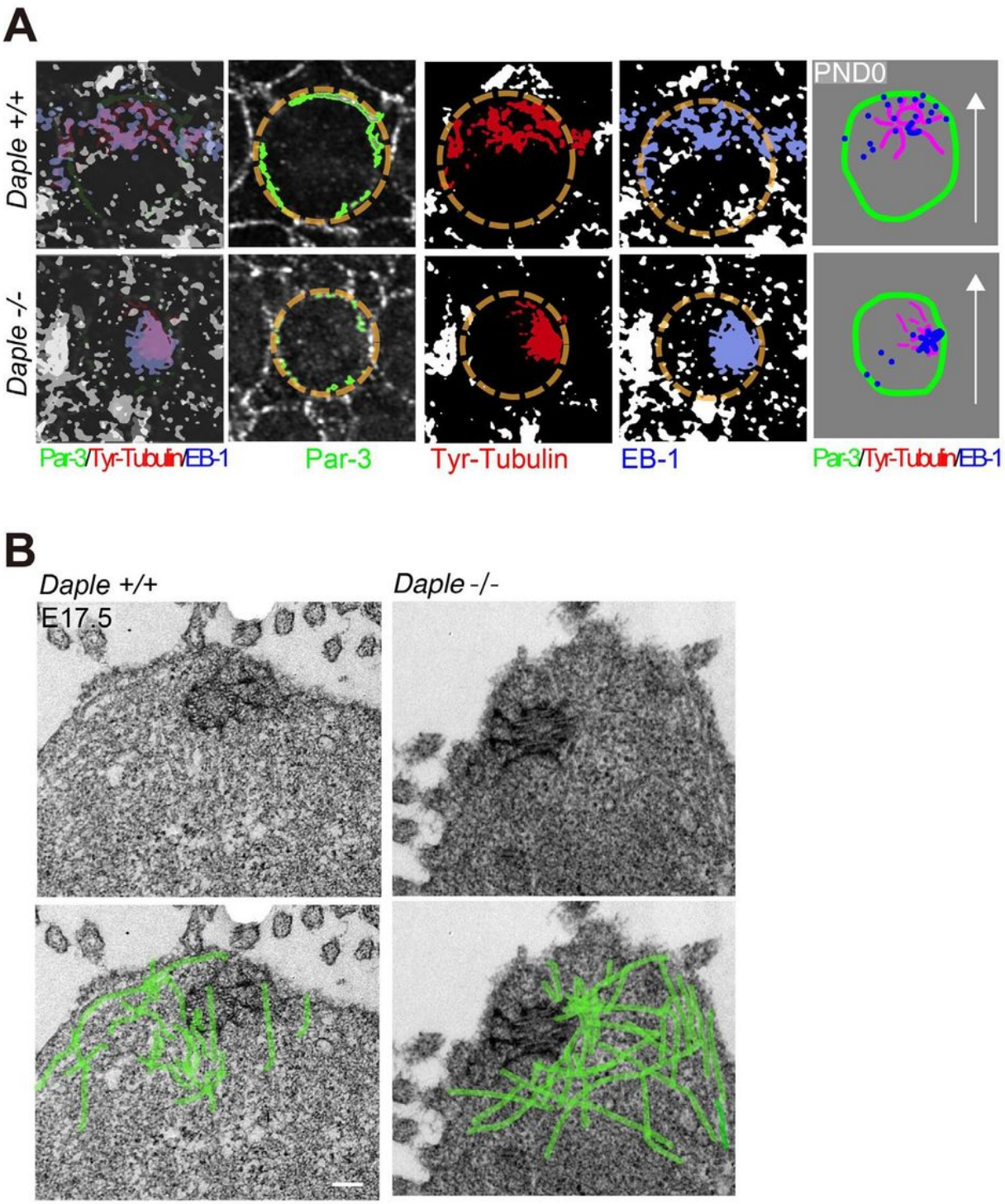

Figure 5

EB-1/Tyr-tubulin staining and transmission electron microscopy (TEM) images (A) Images of EB-1/Tyr-tubulin staining from Figure.4C processed using PhotoShop. The distribution of EB-1, a microtubule plus-end binding protein, was observed near the lateral membrane of hair cells (HCs) in Daple+/+ mice; however, EB-1 in Daple-/- HCs was more densely aggregated in the cytoplasm. (B) The microtubular network extending from the basal body was clearly obsserved in murine Daple+/+ HCs. However, the microtubules showed a higer dense distribution around basal bodies in Daple-/-mice. Scale bar: 1 μm.

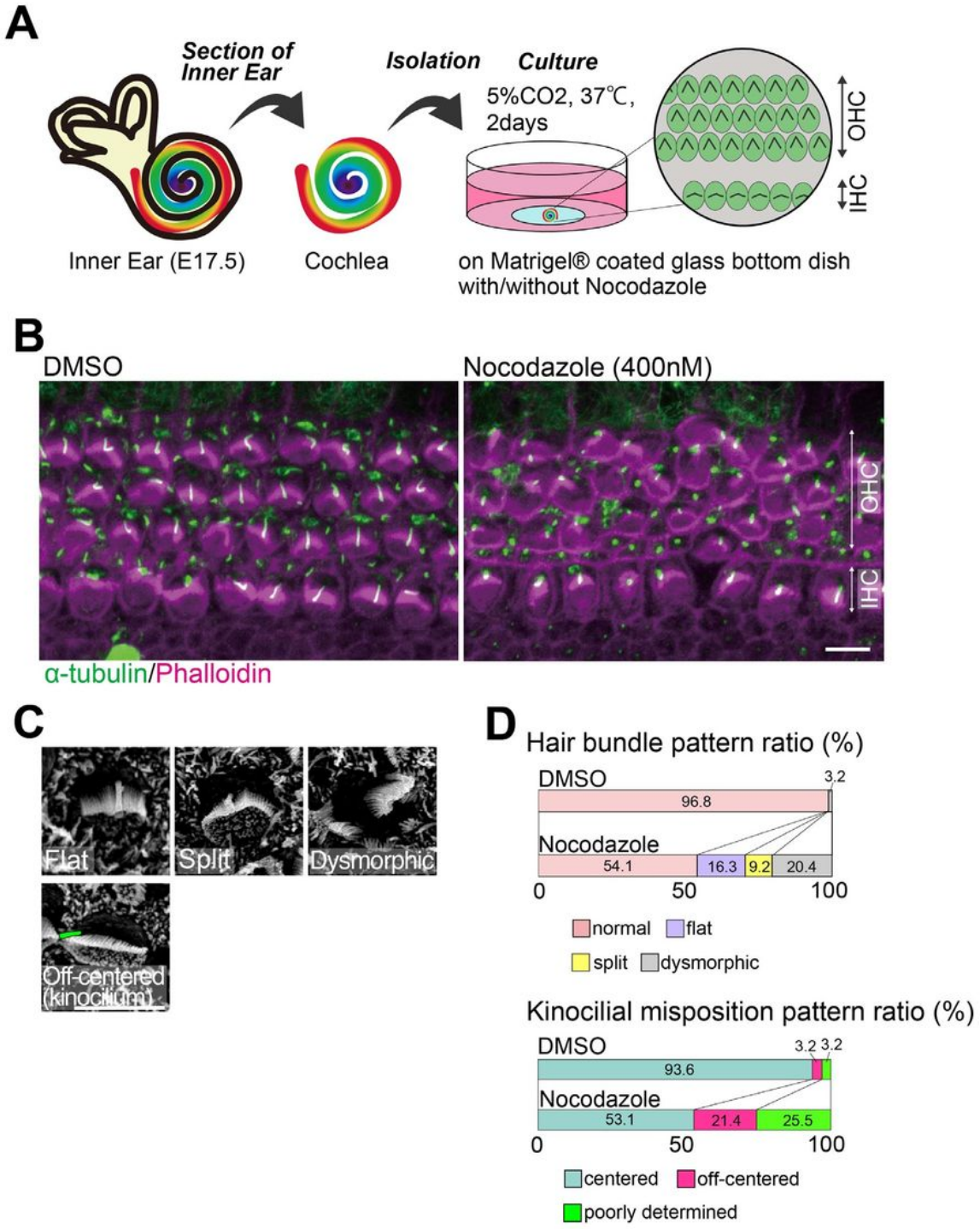

Figure 6

Cochlear organ culture with nocodazole treatment (A) We performed embryonic day (E)17.5 mouse cochlear organ culture. (B) After treatment with 0.05% DMSO or 400 nM nocodazole for 2 days, we performed immunostaining analyses against α-tubulin (green) and phalloidin (magenta). Many stereocilia bundles showed dysmorphic patterns. (C) In scanning electron microscopy (SEM) images, some stereocilia showed mis-shaped and off-centered patterns after nocodazole treatment. (D) To understand any statistical differences between the two groups (cochlear organ culture started at E17.5,DMSO 80 cells, 400 nM nocodazole 98 cells), we counted and summarized them in (D).

Supplementary Files

This is a list of supplementary files associated with this preprint. Click to download.

- OzonoetalSupplementaryInformationSR.pdf